Journal of Alloys and Compounds 509 (2011) 4308–4313

Contents lists available at ScienceDirect

Journal of Alloys and Compounds

journal homepage: www.elsevier.com/locate/jallcom

Microstructure and texture evolution of the cold-rolled AZ91 magnesium alloy strip under electropulsing treatment

Yanbin Jiang[a,*], Guoyi Tang[b,*], Chanhung Shek[c], Wei Liu[d]

[a] Key Laboratory for Advanced Materials Processing (MOE),University of Science and Technology Beijing, Beijing 100083, China
[b] Advanced Materials Institute, Graduate School at Shenzhen, Tsinghua University, Shenzhen 518055, China
[c] Department of Physics and Materials Science, City University of Hong Kong, 83 Tat Chee Avenue, Kowloon Tong, Hong Kong, China
[d] Laboratory of Advanced Materials, Department of Materials Science and Engineering, Tsinghua University, Beijing 100084, China

ARTICLE INFO

Article history:
Received 3 September 2010
Received in revised form 4 January 2011
Accepted 7 January 2011
Available online 14 January 2011

Keywords:
AZ91 magnesium alloy
Electropulsing
Recrystallization
Texture

ABSTRACT

The effect of electropulsing treatment (EPT) on the microstructure and texture evolution of the cold-rolled AZ91 magnesium alloy strip was investigated using X-ray diffraction (XRD) and electron backscattered diffraction patterns (EBSD). The results indicated that EPT accelerated tremendously the recrystallization behaviour of the cold-rolled AZ91 magnesium alloy strip at a relatively low temperature within a short time of 7 s. It also suppressed precipitation of β-$Mg_{17}Al_{12}$ phase, compared with conventional heat treatment. The recrystallized grains favourably weakened the intensity of the basal texture. A mechanism for rapid recrystallization process during EPT was proposed based on the enhancement of nucleation rate and atomic diffusion resulting from the coupling of the themal and athermal effects.

1. Introduction

Electropulsing treatment (EPT), as an instantaneous high energy input method, has been widely applied for improvement of microstructure and properties of materials. Zhu and co-workers [1–3] reported that EPT-tensile process increased the elongation to failure of a Zn–Al alloy remarkably, and the relationship between the elongation and the electropulsing was discussed from the point of view of dislocation dynamic and microstructure evolution. Wang and Song [4,5] studied the effect of EPT on the mechanical properties of cold-rolled TA15 titanium alloy sheet. They found that EPT induced the local recrystallization and the effect of the damage healing in the TA15 sheet, which significantly increased the total elongation. Zhou et al. [6] indicated that direct current accelerated the growth of $TiNi_3$ and TiNi layer because the current could decrease the growth activation energy of the whole interfacial layer. Liu et al. [7] found that EPT could enhance shape memory effect of Fe-based shape memory alloy owe to accelerating the precipitation of NbC carbide particles under EPT. Wang also et al. [8] found that direct current could accelerate the aging process of Cu–Cr–Zr alloy due to the promotion of diffusibility of the solute atoms and the mobility of vacancies. Recently, Xu et al. and Guan et al. [9–11] have succeeded in obtaining ultrafine recrystallized grains in a cold-rolled AZ31 strips by using EPT. The recrystallization behaviour under EPT could be attributed to the promotion of the dislocation movement and annihilation as well as enhancement of grain boundary migration. Du et al. [12] also reported that EPT leaded to recrystallized grains in ECAPed AZ31 alloy by accelerating the motion of dislocations due to the thermal compressive stress. However, the understanding of the detailed mechanism pertaining to the effect of EPT on recrystallization behaviour of Mg alloys is still unclear.

Little has been studied on the effects of conventional annealing on the cold-worked AZ91 magnesium alloy, as a supersaturated solid-solution, because the competitive behaviour between β phase precipitation and recrystallization of α-Mg matrix is complex. Effects of EPT on cold-rolled AZ91 alloy has not been reported either. The present work was initiated to study the effect of EPT on the microstructure evolution of the cold-rolled AZ91 alloy strip and the mechanism of the effect is discussed.

2. Experimental procedures

A commercial magnesium alloy AZ91 (9.1 wt% Al, 0.9 wt% Zn, 0.2 wt% Mn, balance Mg) was used in this investigation. The ingot was homogenized at 673 K for 16 h and subsequently extruded into strip of width 2.90 mm and thickness of 1.45 mm. The extruded strip was cold-rolled to 1.20 mm thick, following by solid solution treatment to obtain supersaturated AZ91 alloy. The strip after the solid solution treatment was further cold-rolled into 0.96 mm thick, viz. 20% cold reduction. The cold-rolled strips were then subjected to EPT with various parameters of electropulsing, as listed in Table 1. For comparison, the cold-rolled strip was heated up to 630 K

* Corresponding authors.
E-mail addresses: jyb05@mails.tsinghua.edu.cn (Y. Jiang), tanggy@mail.tsinghua.edu.cn (G. Tang).

0925-8388/$ – see front matter © 2011 Elsevier B.V. All rights reserved.
doi:10.1016/j.jallcom.2011.01.052

Table 1
Electric parameters of EPT subjected to the cold-rolled AZ91 strip.

Sample no	Frequency f (Hz)	Duration τ_p (μs)	j_m (A/mm^2)	I_e (A)	Measured temperature near the cathode T (K)
EPT1	60	70	362	55.2	411
EPT2	70	70	362	61.0	431
EPT3	85	70	362	65.7	460
EPT4	100	70	362	70.1	482
EPT5	110	70	366	74.9	501
EPT6	121	70	366	79.1	526
EPT7	133	70	367	83.8	563

Note: j_m is the amplitude of current density of electropulsing.
I_e represents the RMS value of current during EPT and is related to the Joule heating effect.

in about 8 s in a furnace, followed by natural cooling in air. The average heating rate was about 45 K/s, and this simulated the thermal effect during EPT. This sample was referred to as sample AT.

The EPT process is schematically shown in Fig. 1. The AZ91 strip was on-line treated by multiple electropulses, when the strip was moving at a speed of 2 m/min through a distance of 225 mm between the two electrodes. Multiple electropulses were continuously produced by a self-made electropulsing generator. During this process, it took about 7 s for the strip to travel from the anode and the cathode. The pressure between the electrodes and the strip was just sufficient to keep good electrical contact without causing deformation of the strip. Electropulses with various frequencies and pulse duration of about 70 μs were applied to the strip. The current parameters including frequency, root-mean-square current (RMS), amplitude and duration of current pulses were monitored by a Hall effect sensor connected to an oscilloscope. The temperature of the AZ91 strip near the cathode was measured using a Raytek MX2 infrared thermoscope, which was calibrated repeatedly with thermocouple prior to temperature measurement.

The samples for both optical microscopy (OM) and EBSD orientation mapping (OIM) were cut out from the central part of the strip. The samples were polished and etched in picric acid for optical observation, and electrolytically polished for EBSD orientation mapping. EBSD analysis was performed on a TESCAN-SEM equipped with an HKL-EBSD system. OIM maps were measured in a unit area of 300 μm × 300 μm and the scan step length was set to be 0.5 μm. The phases in the samples were identified by X-ray diffraction (XRD) using a Philips X'Pert diffractometer with Cu K_α radiation. Vickers hardnesses of all the samples were measured as well.

3. Results

The relationship between hardness, temperature measured near the cathode and frequency of EPT is shown in Table 1 and Fig. 2. It was found that the temperature of the EPT samples increased gradually with frequency due to the Joule heating effect [13,14]. On the other hand, hardness of the samples decreased gradually with an increase in frequency. Especially, the decrease in hardness was abrupt at the frequency of 110 Hz. This means that EPT induced the softening effect of the cold-rolled AZ91 alloy progressively with an increase in frequency of electropulsing.

Fig. 3 shows the XRD patterns of the cold-rolled sample and the EPT samples. Since the cold-rolled sample was a supersaturated solid solution prior to cold-rolling, only the α-Mg peak appeared in its XRD pattern. After EPT, the weak β-$Mg_{17}Al_{12}$ phase peak appeared and the intensity increased slightly with frequency of EPT, as indicated by the solid squares in Fig. 3. However, the β-$Mg_{17}Al_{12}$ phase peak gradually weakened and vanished when frequency exceeded 100 Hz. This implies that with increasing frequency of EPT, a small amount of β-$Mg_{17}Al_{12}$ phase were formed initially in the α-Mg matrix and then redissolved into α-Mg matrix.

Fig. 4(a) shows the optical microstructure of the cold-rolled sample, which exhibits typical cold-rolled structure of Mg alloy, with many deformation twins inside the grains of average size of about 45 μm. The EBSD orientation mapping of the samples

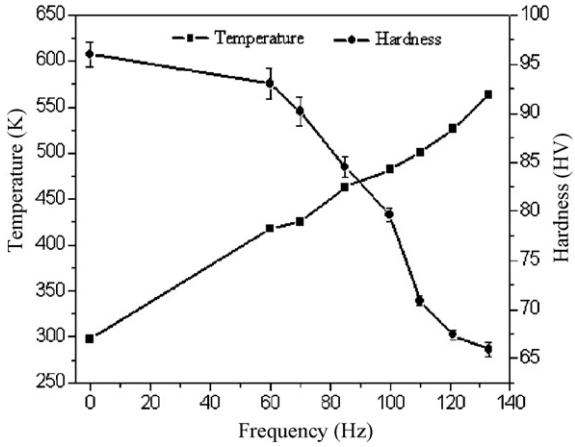

Fig. 2. Relationship between hardness, temperature and frequency of electropulsing of samples.

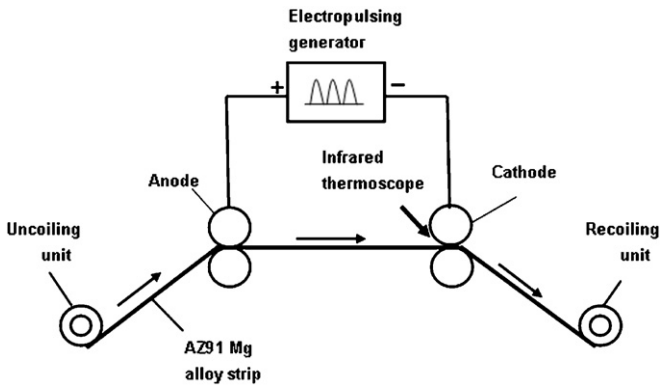

Fig. 1. The schematic view of EPT process.

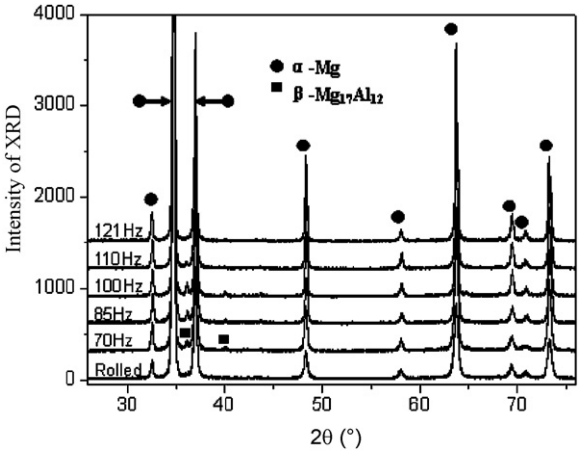

Fig. 3. XRD patterns for samples at various conditions.

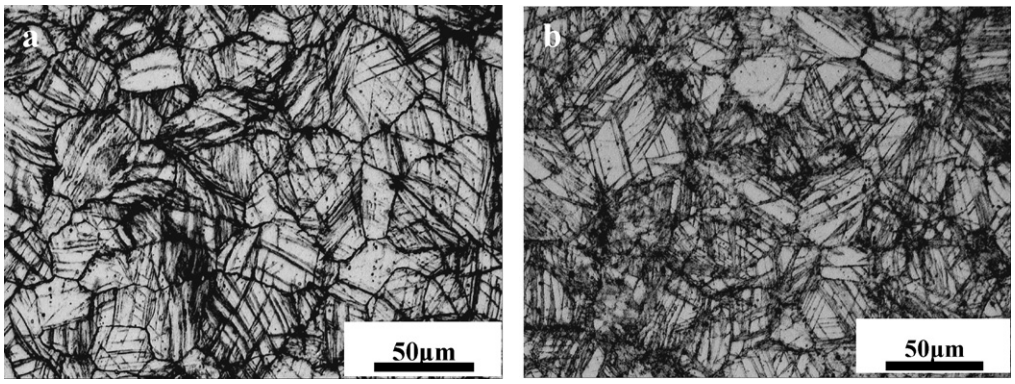

Fig. 4. Optical micrographs of the cold-rolled sample: (a) and sample AT (b).

after EPT are illustrated in Fig. 5, where the high angle boundaries (HAB) with misorientation larger than 15° are labeled by black bold line and the low angle boundaries (LAB) with misorientation within 2–15°are labeled by black fine line. A large number of LAB and fragmented substructures mixed with many deformation twins, appeared in the primary grains of the cold-rolled sample, as shown in Fig. 5(a). After 100 Hz-EPT, new fine recrystallized grains nucleated preferentially at the high-strain region (grain boundaries and deformation bands, etc.). Furthermore, some nucleus were formed inside twins and tended to grow along the twin boundaries into long and thin grains, as shown in Fig. 5(b). When frequency was increased to 110 Hz, recrystallization was completed and all the primary grains were consumed by many fine recrystallized grains with average size of about 6 μm, as shown in Fig. 5(c). With further increasing frequency to 133 Hz, apparent grain growth occurred and relatively homogeneous microstructure of equiaxed grains with average size of about 24 μm was obtained, as shown in Fig. 5(d). In order to simulate the rapid heating during EPT, the cold-rolled AZ91 strip was heated up to about 630 K in about 8 s in a furnace followed by natural cooling in air. The heating rate was close to that of the 133 Hz-EPT sample. However, it was found that the microstructure of the sample AT by rapid heating treatment was similar to that of the cold-rolled sample, as shown in Fig. 4(b). Referring to Table 1 and Fig. 5, it is indicated that EPT tremendously accelerated recrystallization process of the cold-rolled AZ91 alloy strip at relatively low temperature as well as suppressed the precipitation of the β-$Mg_{17}Al_{12}$ phase, compared with conventional heat treatment.

Fig. 6 shows the textures of the samples after EPT. For ease analysis, both $\{0001\}$ and $\{10\bar{1}0\}$ pole figures corresponding to OIM maps in Fig. 5 are illustrated. Normal direction (ND) was vertical to the rolling plane. The cold-rolled sample

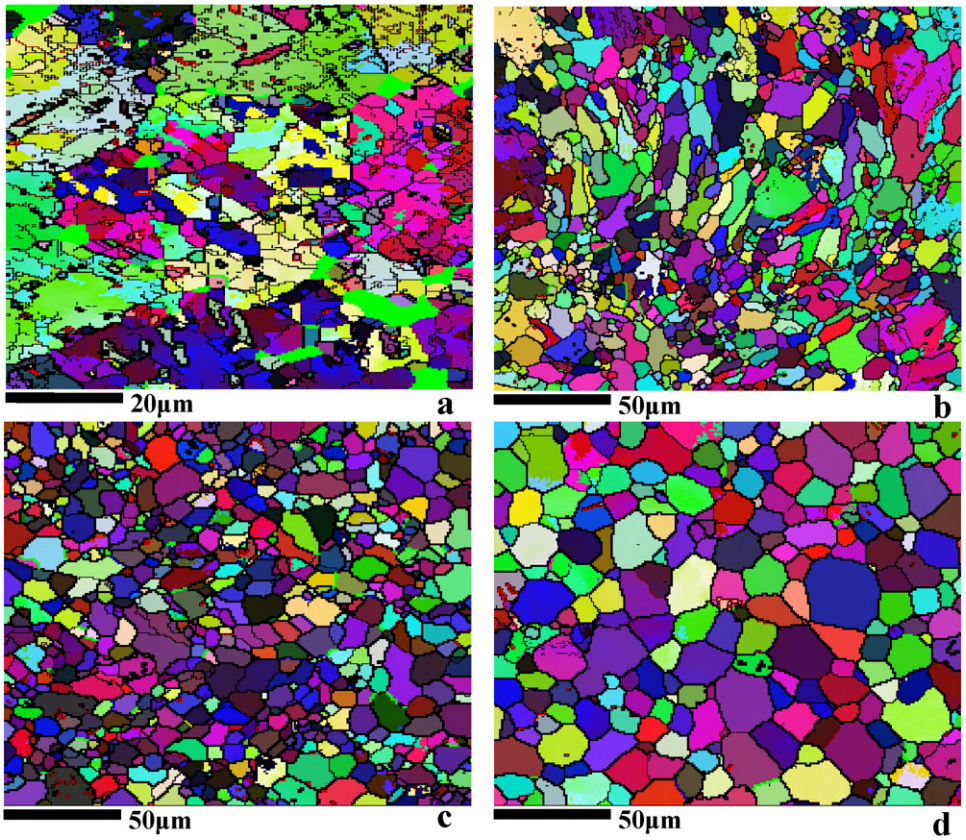

Fig. 5. Orientation map of the AZ91 alloy after EPT: (a) cold-rolled sample; (b) 100 Hz-EPT; (c) 110 Hz-EPT; (d) 133 Hz-EPT.

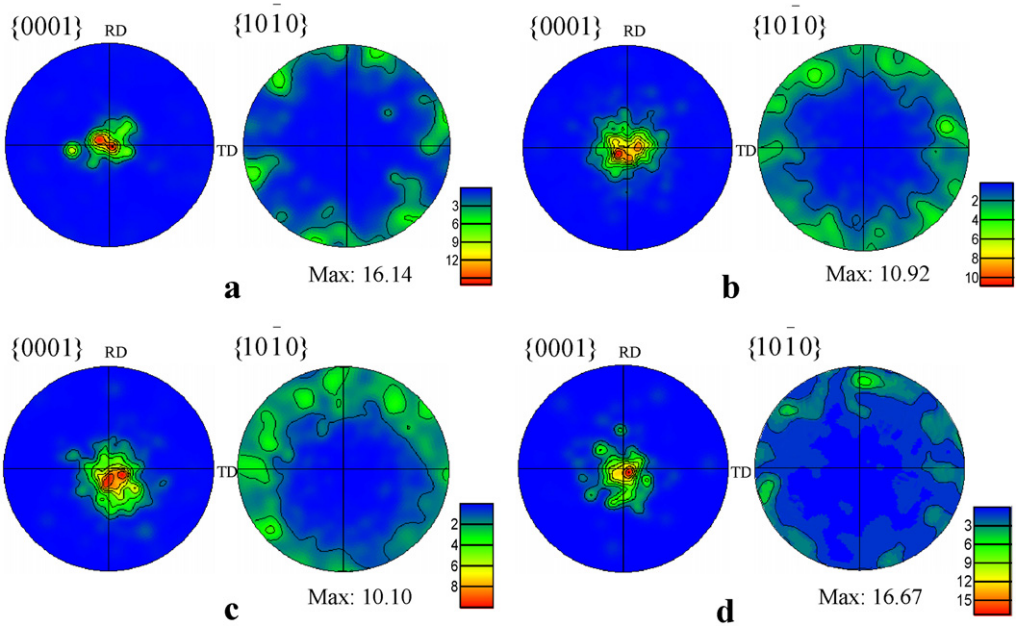

Fig. 6. The $\{0001\}$ and $\{10\bar{1}0\}$ pole figures of the AZ91 alloy after EPT: (a) cold-rolled sample; (b) 100 Hz-EPT; (c) 110 Hz-EPT; (d) 133 Hz-EPT

exhibited a strong $\{0001\}$ basal texture. With increasing frequency to 110 Hz, recrystallization induced by EPT weakened the $\{0001\}$ basal texture gradually until full recrystallization was achieved. With further increasing frequency to 133 Hz, however, the intensity of $\{0001\}$ basal texture increased gradually during EPT induced normal grain growth, accompanying the crystallographic orientation of $\langle 10\bar{1}0 \rangle$ parallel to rolling direction. Fig. 7 shows the misorientation angle distribution of the EBSD samples. The cold-rolled sample consisted of mainly two misorientation angle distribution peaks of 2–10° and 85–90°. With increasing frequency, the amount of the misorientation angle distribution of 2–10° and 85–90° decreased gradually and a broad

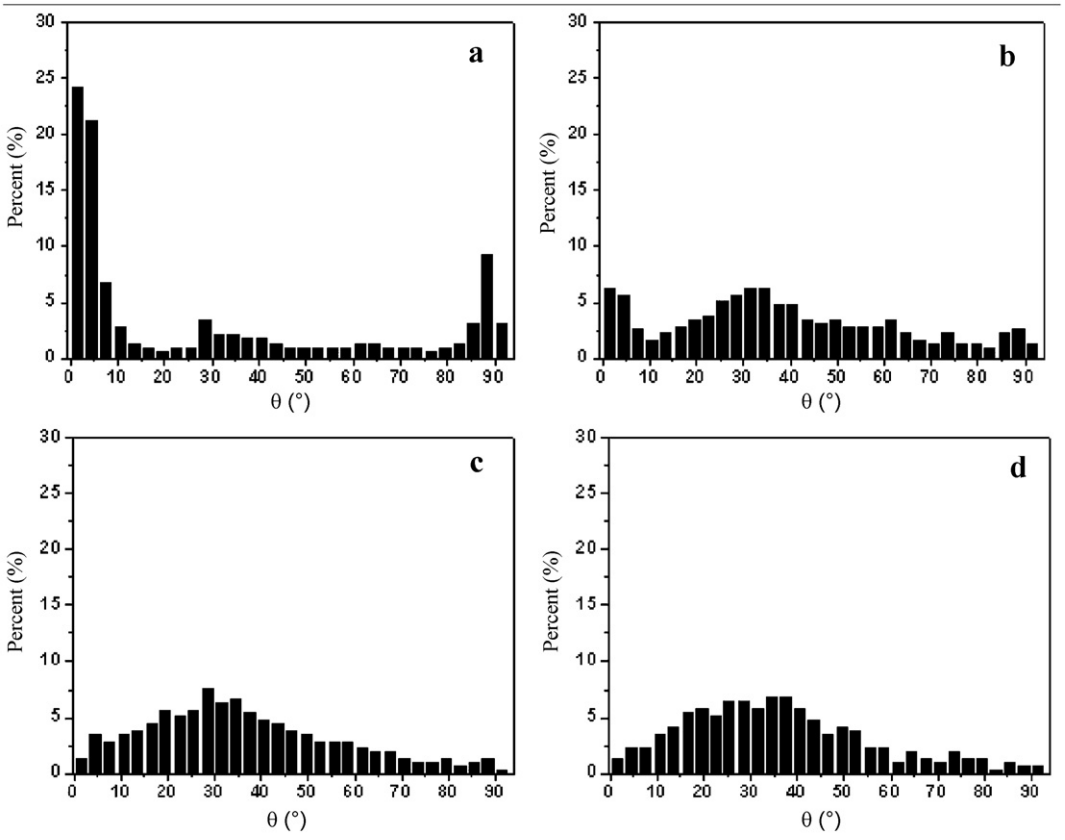

Fig. 7. Misorientation angle distribution of the AZ91 alloy after EPT: (a) cold-rolled sample; (b) 100 Hz-EPT; (c) 110 Hz-EPT; (d) 133 Hz-EPT

misorientation angle distribution in the range of 15–60° became predominant.

4. Discussion

The intensive $\{0\,0\,0\,1\}$ basal texture appeared in the cold-rolled sample due to the occurrence of the basal slip of dislocations during the cold-rolling process [15–17]. A great number of the basal-type dislocations piled up at grain boundaries,which induced large stress concentration around grain boundaries. These dislocations rearranged themselves to form high density of low angle boundary for releasing stress concentrations [18]. In addition, the misorientation angle distribution of 85–90° existed in the sample because of the twinning of Mg alloy during cold-rolling process [19]. After EPT, the extent of recrystallization increased gradually and the full-recrystallized microstructure of fine equiaxed grains could be obtained with an increase in frequency of electropulsing, which induced the decrease in hardness of the samples. The intensity of the basal texture decreased mainly due to the formation of new recrystallized grains with other crystallographic misorientation. From the analysis of the misorientation angle distribution of the EPT samples, it is indicated that EPT completed the transition from low angle grain boundary to high angle grain boundary by promoting rearrangement of dislocations during a short time of 7 s, which favourably accelerated recrystallization process of the AZ91 alloy. The disappearance of the misorientation angle distribution peaks of 85–90° indicated indirectly that some recrystallized grains were probably formed inside the twins and further grew to consume the primary twins, which was observed in Fig. 5(b).

The XRD analysis shows that a small amount of β-$Mg_{17}Al_{12}$ phase precipitated initially in the α-Mg matrix and then redissolved into the matrix with an increase in frequency of electropulsing. Both precipitation and dissolution of β-$Mg_{17}Al_{12}$ phase depend critically on the diffusion of Al atom in the AZ91 alloy. Our previous studies [13,14,20,21] indicated that EPT tremendously accelerated the diffusion of Al atom due to the coupling of the thermal and athermal effects. Therefore, a small quantity of β-$Mg_{17}Al_{12}$ phase was formed at the region of high strain during EPT with low frequency. With increasing frequency of EPT, the rapid temperature rise induced by Joule heating effect remarkably reduced the driving force for precipitation of β-$Mg_{17}Al_{12}$ phase, and even caused redissolution of the β-$Mg_{17}Al_{12}$ phase. It is worth noting that the β-$Mg_{17}Al_{12}$ phase almost disappeared completely when recrystallization was completed under EPT with frequency of 110 Hz, as shown in Figs. 3 and 5(c).

During recrystallization, the kinetics of EPT induced recrystallization should be taken into account. It is well known that recrystallization kinetics depends on the nucleation rate and growth rate of recrystallization nuclei [22]. Nucleation is generally involved by the formation and growth of subgrains via dislocation rearrangement (movement and annihilation of dislocations, etc) during conventional annealing process. It is supposed that the nucleation rate could be increased by promoting dislocation rearrangement during annealing process. For the sample AT, the deformed microstructure still existed and no apparent recrystallization behaviour was found. However, EPT with frequency of 110 Hz completed recrystallization process of the cold-rolled AZ91 alloy at the relatively low temperature within a short time of 7 s. This implies that EPT effectively accelerated recrystallization process by substantially promoting dislocation motions. Previous studies [23–25] indicated that an additional force formed by the periodic impulse electrons of electropulsing, known as “electron wind”, exerted on dislocations, which favourably promoted the dislocation motions. Guan et al. [10] proposed that EPT accelerated recrystallization process by enhancing boundary migration due to an additional driving force of electropulsing. However, the exact mechanism of how electropulsing affects the recrystallization behaviour is still not clear. Here, one possible explanation for the effect of EPT on recrystallization behaviour of the AZ91 alloy is based on the promotion of dislocation climb resulting from the coupling of the thermal and athermal effects. Previous studies [26] reported that dislocation climbing into subgrain boundary was closely related to the total atomic flux. During multiple continuous electropulsing through the AZ91 strips, the average atomic flux per second can be described by Eq. (1):

$$J^{\mathrm{r}} = J_{\mathrm{t}}^{\mathrm{r}} + J_{\mathrm{a}}^{\mathrm{r}} = \frac{\pi G b D_{\mathrm{l}}}{(1-\nu)kT} + \frac{2N D_l Z^* e \rho f j_{\mathrm{m}} \tau_{\mathrm{p}}}{\pi k T} \quad (1)$$

$$J_{\mathrm{t}}^{\mathrm{r}} = \frac{\pi G b D_l}{(1-\nu)kT} \quad (2)$$

$$J_{\mathrm{a}}^{\mathrm{r}} = \frac{2N D_l Z^* e \rho f j_{\mathrm{m}} \tau_{\mathrm{p}}}{\pi k T} \quad (3)$$

where J^{r} is the total flux of atom under EPT, $J_{\mathrm{t}}^{\mathrm{r}}$ the flux of atom resulting from the thermal activated effect of EPT [27], $J_{\mathrm{a}}^{\mathrm{r}}$ the flux of atom contributed by the athermal effect of EPT [13], G the shear modulus, b the Burgers vector, ν Poisson's ratio, N the density of atoms, Z^* effective valence of the Mg ion, e the charge on an electron, ρ the electrical resistivity, k the Boltzmann constant, T the absolute temperature, D_{l} the lattice diffusion coefficient; j_{m}, f, and τ_{p} are peak current density, frequency and duration of electropulsing, respectively.

According to Eq. (1), EPT tremendously increases the average atomic flux compared with conventional heat treatment due to the athermal effect of electropulsing, which is an additional high energy input through momentum transferred from electrons. This implies that with the aid of electropulsing the average atomic flux is adequate to accelerate recrystallization process by substantially promoting dislocation rearrangement at a relatively low temperature in a short time of 7 s. Furthermore, Eq. (1) reveals that $J_{\mathrm{a}}^{\mathrm{r}}$ increases linearly with the three electric parameters, j_{m}, f, and τ_{p} Under EPT, temperature of the sample increases with these three parameters because increasing j_{m}, f, and τ_{p} results in the larger Joule heating effect. As a result, increasing, f, τ_{p} and j_{m} not only increases the athermal effect but also increases the thermal effect. Additionally, temperature of the samples is a very important factor under EPT, which can be demonstrated by the microstructure evolution of the samples after EPT with only change in the frequency of electropulsing. Actually, many non-recrystallized grains were observed, termed as incomplete recrystallization, in the sample after 100 Hz-EPT. However, by only increasing frequency to 110 Hz or 133 Hz, the full recrystallization could be achieved and the subsequent grain growth occurred, respectively. It is apparent that increasing frequency enhances the atomic flux due to the athermal effect in Eq. (1). Nevertheless, as long as only the effect of frequency on the atomic flux was considered, the completion of recrystallization cannot be explained satisfactorily because the electropulsing frequency change of 10 Hz or 33 Hz would not affect the athermal effect much, as shown in Eq. (1). In fact, temperature is another important factor for the atomic flux in the case of EPT since D_{l} increases exponentially with temperature T in the Eq. (4) [28]:

$$D_{\mathrm{l}} = D_0 \exp(-\frac{Q}{RT}) \quad (4)$$

where D_0 is the diffusion pre-exponential factor, Q the activation energy, R gas constant. Based on the above analysis, EPT tremendously accelerated recrystallization process due to the enhancement of atomic flux at an adequate temperature. With further increasing frequency (above 110 Hz), the rapid temperature rise resulting from Joule heating effect resulted in the apparent grain growth of Mg matrix.

In the present study, the mechanism of EPT induced recrystallization was mainly based on the enhancement of the atomic flux due to the coupling of the thermal and athermal effects of EPT. However, further clarification of the exact mechanism of EPT on the recrystallization kinetics should be conducted in the future, including the analysis of the relative contributions of J_t^r and J_a^r.

5. Conclusions

EPT induced recrystallization of cold-rolled AZ91 strip, and suppressed the precipitation of β-$Mg_{17}Al_{12}$ phase in the α-Mg matrix, at a relatively low temperature within a short time of 7 s, while no apparent recrystallization behaviour was found in conventional heat treatment with similar heating profile as EPT.

The extent of EPT induced recrystallization increased gradually with frequency, and the recrystallized grains favourably weakened the intensity of the basal texture until the full recrystallization was achieved. Further increasing frequency of EPT resulted in grain growth due to the high temperature, accompanying the increasing intensity of basal texture.

Compared with conventional heat treatment, EPT tremendously accelerated recrystallization process of the cold-rolled AZ91 due to the substantial increase in the atomic flux resulted from the coupling of the thermal and athermal effects. An adequate thermal effect resulted from Joule heating of EPT should be needed for an effective operation of the athermal effect resulted from the interaction between electrons and atoms.

Acknowledgements

Authors would like to thank the support from the Tsinghua-CityU Collaboration Scheme. The work was supported by the National Natural Science Foundation of China (No. 50571048) and a Strategic Research Grant (Grant No. 7002303) from City University of Hong Kong. We also thank Dr. ZH. Xu for providing the extruded AZ91 strip.

References

[1] Y.H. Zhu, S. To, W.B. Lee, X.M. Liu, Y.B. Jiang, G.Y. Tang, Mater. Sci. Eng. A 501 (2009) 125–132.
[2] S. To, Y.H. Zhu, W.B. Lee, X.M. Liu, G.Y. Tang, Y.B. Jiang, Mater. Trans. 50 (2009) 1105–1112.
[3] S. To, Y.H. Zhu, W.B. Lee, X.M. Liu, Y.B. Jiang, Mater. Trans. 50 (2009) 2772–2777.
[4] Z. Wang, H. Song, J. Alloys Compd. 470 (2009) 522–530.
[5] Z. Wang, H. Song, Trans. Nonferrous Met. Soc. China 19 (2009) 409–413.
[6] Y. Zhou, Q. Wang, D.L. Sun, X.L. Han, J. Alloys Compd. 509 (2011) 1201–1205.
[7] W.B. Liu, Y.H. Wen, N. Li, S.Z. Yang, J. Alloys Compd. 472 (2009) 591–594.
[8] Z.Q. Wang, Y.B. Zhong, Z.S. Lei, W.L. Ren, Z.M. Ren, K. Deng, J. Alloys Compd. 471 (2009) 172–175.
[9] Z.H. Xu, Tang.F G.Y, F. Ding, S.Q. Tian, H.Y. Tian, Appl. Phys. A 88 (2007) 429–433.
[10] L. Guan, G.Y. Tang, Y.B. Jiang, P.K. Chu, J. Alloys Compd. 487 (2009) 309–313.
[11] L. Guan, G.Y. Tang, P.K. Chu, Y.B. Jiang, J. Mater. Res. 24 (2009) 3674–3679.
[12] X.N. Du, S.M. Yin, S.C. Liu, B.Q. Wang, J.D. Guo, J. Mater. Res. 23 (2008) 1570–1577.
[13] Y.B. Jiang, G.Y. Tang, L. Guan, S.N. Wang, C.H. Shek, Z.H. Xu, Y.H. Zhu, J. Mater. Res. 23 (2008) 2685–2691.
[14] Y.B. Jiang, G.Y. Tang, C.H. Shek, Y.H. Zhu, L. Guan, S.N. Wang, Z.H. Xu, J. Mater. Res. 24 (2009) 1810–1814.
[15] M.T. Prado, J.A. Valle, J.M. Contreras, O.A. Ruano, Scripta Mater. 50 (2004) 661–665.
[16] L. Wagner, M. Hilpert, J. Wendt, B. Kuster, Mater. Sci. Forum 419–422 (2003) 93–102.
[17] R. Poss, Mater. Sci. Forum 419–422 (2003) 327–336.
[18] H.L. Ding, L.F. Liu, S. Kamado, W.J. Ding, Y. Kojima, Mater. Sci. Eng. A 452–453 (2007) 503–507.
[19] J. Jiang: Research on influence of initial texture and temperature on compression plastic behaviour of AZ31 magnesium alloy. Ph.D. Thesis, Beijing, Tsinghua University, 2008, p.101.
[20] Y.B. Jiang, G.Y. Tang, C.H. Shek, Y.H. Zhu, Appl. Phys. A 97 (2009) 607–615.
[21] Y.B. Jiang, G.Y. Tang, C.H. Shek, Y.H. Zhu, Z.H. Xu, Acta Mater. 57 (2009) 4797–4808.
[22] F.J. Humphreys, M. Hatherly, Recrystallization and Related Annealing Phenomema, 2nd ed., Elsevier, Amsterdam, 2004.
[23] F.R. Nabarro, Theory of Crystal Dislocations, Clarendon Press, Oxford, 1967.
[24] V.Y. Kravchenko, Sov. Phys. Solid State 8 (1966) 740–745.
[25] V.Y. Kravchenko, JETP 24 (1967) 1135–1142.
[26] Z.Y. Liu, X.T. Deng, Y.Z. Weng, Chin. J. Mater. Res. 15 (2001) 358–364 (in Chinese).
[27] Y.N. Xu, W.M. Mao, Structure of Materials, Metallurgy industry press, Beijing, 2001.
[28] D.A. Porter, K.E. Easterling, Phase Transformations in Metals and Alloys, 2nd ed., Chapman.Hall, London, 1992.